Journal of Alloys and Compounds 509 (2011) 3387–3392

Contents lists available at ScienceDirect

Journal of Alloys and Compounds

journal homepage: www.elsevier.com/locate/jallcom

Microstructure evolution and modification mechanism of the ytterbium modified Al–7.5%Si–0.45%Mg alloys

Bao Li[a,*], Hongwei Wang[b], Jinchuan Jie[a], Zunjie Wei[a,*]

[a] School of Materials Science and Engineering, Harbin Institute of Technology, Harbin 150001, PR China
[b] National Key Laboratory of Precision Hot Processing of Metals, Harbin Institute of Technology, Harbin 150001, PR China

ARTICLE INFO

Article history:
Received 13 August 2010
Received in revised form 9 December 2010
Accepted 10 December 2010
Available online 21 December 2010

Keywords:
Hypoeutectic Al–Si alloy
Eutectic solidification
Microstructure
Modification
Ytterbium

ABSTRACT

The effects of ytterbium (Yb) on the microstructure and eutectic solidification behavior of Al–7.5%Si–0.45%Mg alloys were investigated. Samples with different contents of Yb were quenched just after the commencement of eutectic arrest. Microstructures of the as-cast and quenched samples were examined by optical microscopy (OM) and scanning electron microscopy (SEM). The microstructural observations show that the addition of Yb causes a structural transformation of eutectic silicon from a coarse plate to a fine flake-like and some branched morphology. In addition, the formation of Yb-containing phases at higher content of Yb results in a deterioration of modification. Furthermore, the results of thermal and quenching analysis reveal that the addition of Yb reduces the temperatures of eutectic nucleation and growth. The growth rather than nucleation of eutectic is thought to be the primary cause of modification, and the corresponding undercooling caused by the presence of Yb plays an important role in the refinement of eutectic silicon.

1. Introduction

The hypoeutectic Al–Si alloys are extensively used in the automotive and aerospace industries because of the excellent properties including castability, weldability, corrosion resistance and integrated mechanical properties [1,2]. Silicon is a faceted phase and makes the Al–Si eutectic an irregular eutectic. The brittleness of silicon crystals, of course, is the main reason responsible for the poor properties of Al–Si alloys since the large eutectic silicon particles lead to premature crack initiation and fracture in tension conditions [1].

It has been proven that modification of eutectic silicon plays an important role in improving the mechanical properties of hypoeutectic Al–Si alloys, particularly the elongation. Therefore, many efforts have been made in the modification of casting Al–Si alloys in order to achieve fine silicon phase with beneficial shapes and distribution. The eutectic silicon in Al–Si alloy can be modified using chemical [3], quenching [4,5], outfield [6,7], or superheating modification [8,9]. The most common chemical elements used in industry today are Na and Sr [3], which change silicon from coarse plate-like to a fine fibrous structure, and Sb [4,10] which only causes a refinement in the flake-like silicon structure. It is also reported that some rare earth (RE) elements, including La [11], Eu [12,13], Yb [12,14], Y [14–16] and Sc [17,18] can change the Al–Si eutectic from a coarse plate or flake to a fibrous or laminar morphology.

Various theories were proposed for the exact mechanism of modification, including restricted nucleation theory and restricted growth theory [19]. Although the parameters such as crystal structure, lattice constant, melting point, vapour pressure and mixing enthalpy [20] were reported for the selection of silicon modifying agents in the Al–Si system, the most widely accepted theory is the impurity induced twinning model (IIT) [21]. The model suggests that a high density of twinning occurs in silicon in the modified alloys because atoms of the modifier are absorbed onto the growth steps of the silicon solid–liquid interface. However, there are a few dissenting publications about the effect of RE on eutectic modification in hypoeutectic Al–Si alloys [21–23]. The IIT mechanism that addition of modifying agent alters the growth of the silicon phase during solidification is now widely contested [24]. Although twins are frequently observed in silicon crystals, twinning is not believed to be the sole effective mechanism of modification. The theory which questions this indicates that there is a relationship between the degree of modification and the nucleation of eutectic phases. It has been proposed that the β-(Al, Si, Fe) phases [25,26] or AlP particles [27–29] play an important role in the nucleation of the eutectic phases in hypoeutectic Al–Si alloys. The modifying agents can poison the active nucleation sites and results in a significant undercooling of the interdendritic liquid at the eutectic temperature, resulting in modification of eutectic silicon [24]. Furthermore, it is also proposed that the addition of modifying agent

* Corresponding author at: School of Materials Science and Engineering, Harbin Institute of Technology, No. 92 Da-zhi Street, Harbin, Heilongjiang Province, PR China. Tel.: +86 451 86403150; fax: +86 451 86418131.
E-mail addresses: libao1983@yahoo.com.cn (B. Li), weizj@hit.edu.cn (Z. Wei).

0925-8388/$ – see front matter © 2010 Elsevier B.V. All rights reserved.
doi:10.1016/j.jallcom.2010.12.081

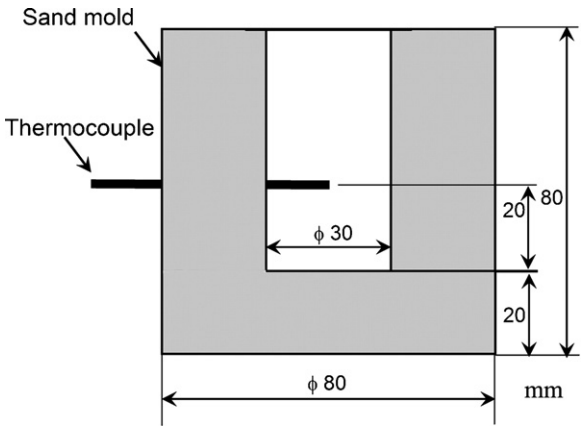

Fig. 1. A schematic diagram of sand mold and thermocouple for thermal analysis (unit: mm).

alters the liquid atomic structure and interfacial energy of the alloy [24,30]. However, these assertions have generated some controversy while the role of the particles remains unresolved [31,32]. The increased interface velocity caused by reduced nucleation is not sufficient to cause a flake–fibrous transition, and the flake-to-fibre transition that occurs with impurity modification is shown to be independent of any change in eutectic nucleation mode and frequency [32]. Therefore, despite decades of research, the exact mechanism of modification is still under debate.

In this paper, a rare earth element Yb was added as a trace additive, which has the most optimal ratio with r/r_{Si} of 1.65 [21] and is likely to be present in the silicon phases [12]. The aim of the present research is therefore to investigate the effects of Yb on the eutectic microstructure of Al–7.5%Si–0.45%Mg alloys, particularly the size and morphology of the eutectic silicon phase. Furthermore, the eutectic solidification behavior of Al–7.5%Si–0.45%Mg alloys was also studied by thermal analysis and quenching experiments.

2. Experimental procedures

Al–7.5%Si–0.45%Mg (all percentages are wt.% unless otherwise stated) alloys about 2 kg were melted in an electrical resistance furnace and the melting temperature was kept at about 730 ± 5 °C. The melt was degassed with high purity argon gas for 30 min using a rotary graphite degasser. Subsequently, the corresponding contents of Yb were added to the melt as small pieces of pure Yb at 730 °C, wrapped in aluminum foil, and the nominal addition levels were between 0.15 and 1.0%. For comparison, the 0.04% Sr addition was used as a reference which is the conventional modifying agent for hypoeutectic Al–Si alloys. The molten metal was manually stirred for a few seconds and then held at 730 °C for about 20 min to ensure homogeneity before pouring.

The surface of the melt was skimmed and then the melt was poured into a cylindrical sand mould (Fig. 1) at about 710 °C, where the alloy was solidified at an average cooling rate of approximately 5 °C/s, just before the first solid was formed. Meantime, the cooling curve was monitored during solidification, as illustrated schematically in Fig. 1. Thermal analysis was performed using a technique similar to that used by Knuutinen et al. [14] to determine eutectic nucleation temperature (T_N), growth temperature (T_G), and minimum temperature (T_{Min}). The characteristic temperature is identified as the point where the cooling curve starts to bend and is found more easily with the use of the derivative of the curve. The difference between T_G and T_{Min} (i.e., $\Delta T = T_G - T_{Min}$) describes the recalescence of the eutectic arrest (ΔT). Quenching experiments were performed during the eutectic arrest to further investigate the nucleation behavior of eutectic silicon. Fig. 2 shows a schematic of the experimental set-up for quenching experiment. Samples were extracted in tapered stainless steel cups as shown in Fig. 2, which were situated in a holding furnace. The sample was allowed to cool until the desired temperature was reached at which time the sample was plunged into the brine bucket at about 5 °C. The chemical compositions of the alloys were measured by a spectrometry (Switzerland, ARL-4460), detailed in Table 1.

The as-cast and quenched samples were sectioned perpendicular to the cylinder axis 15 mm and 5 mm from the base of the cylindrical castings, respectively. Microstructures were examined on a Hitachi S-4700 scanning electron microscopy equipped with an energy dispersive spectroscopy (EDS) after deeply etching for 20 min with a 2 vol.% HF–water solution. The quenched samples were etched with a

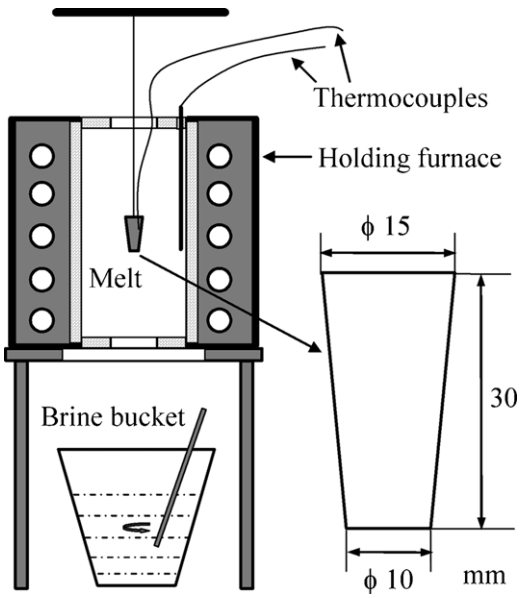

Fig. 2. A schematic diagram of the experimental set-up for quenching experiments (unit: mm).

Table 1
Chemical composition of Al–7.5%Si–0.45%Mg alloys (%).

Alloy	Si	Mg	Fe	P	Sr	Na	Yb	Al
Un	7.34	0.53	0.03	<0.001	<0.005	<0.0005	<0.001	Bal.
0.15Yb	7.41	0.47	0.04	<0.001	<0.005	<0.0005	0.15	Bal.
0.30Yb	7.32	0.44	0.04	<0.001	<0.005	<0.0005	0.28	Bal.
0.50Yb	7.48	0.46	0.03	<0.001	<0.005	<0.0005	0.45	Bal.
1.00Yb	7.44	0.43	0.03	<0.001	<0.005	<0.0005	1.10	Bal.
0.04Sr	7.47	0.49	0.03	<0.001	0.032	<0.0005	<0.001	Bal.

solution (NaOH: 10 g, $K_3Fe(CN)_6$: 5 g, H_2O: 60 ml) for 20–30 s to distinguish primary dendrite, Al–Si eutectic and quenched liquid clearly by optical microscopy.

3. Results

3.1. Microstructure evolution

Microstructures of Al–7.5%Si–0.45%Mg alloys are depicted in Fig. 3, which demonstrate a substantial microstructural difference in the size and morphology of eutectic silicon. Fig. 4 shows the high magnification morphology of eutectic silicon. As shown in Fig. 3a, the microstructure of the unmodified alloy mainly consists of primary aluminum dendrite and eutectic phase with coarse plate-like morphology, typical of Al–Si alloys without any eutectic modification (Fig. 4a). Fig. 3b–e show the eutectic microstructures of Al–7.5%Si–0.45%Mg alloys containing Yb, at the levels of 0.15%, 0.3%, 0.5% and 1.0%, respectively. It is obvious that the size and interflake spacing of eutectic silicon decrease significantly with the addition of Yb. However, the eutectic structure is still flake-like and some branched morphology (Fig. 4b–e), while the 0.04% Sr modified alloy exhibits a fully modified, fine fibrous silicon under the same condition as shown in Figs. 3f and 4f. Furthermore, the eutectic silicon becomes coarser when the content of Yb increases up to 0.5%, but the size of silicon phase is still smaller than that of the unmodified alloy even at 1.0% Yb.

In addition, as the solubility of Yb in Al–7.5%Si–0.45%Mg alloy is comparatively low [33], the Yb-containing phases can be formed in the alloys. At low Yb content, for example 0.15% and 0.3%, few Yb-containing phases can be observed in the microstructure for the small amount and size. But when the content of Yb increases up to 0.5% and 1.0%, the Yb-containing phases can be clearly observed in

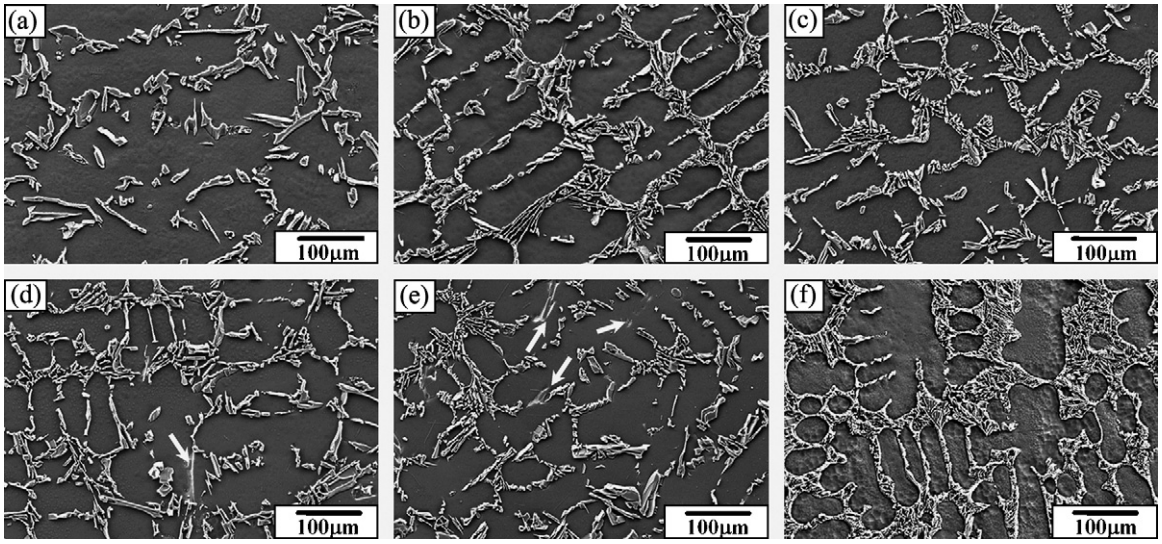

Fig. 3. Microstructures of Al–7.5%Si–0.45%Mg alloys: (a) unmodified, (b) 0.15% Yb, (c) 0.3% Yb, (d) 0.5% Yb, (e) 1.0% Yb and (f) 0.04% Sr.

the microstructure, as highlighted by the arrows in Fig. 3d and e. Fig. 5a shows the typical morphology of Yb-containing phase in the 0.5% Yb modified alloy. The corresponding EDS analysis shows that it contains about 47% Yb, besides Al, Si and Mg, as shown in Fig. 5b. It also reveals that no Yb can be detected in the aluminum matrix, even up to 1.0% Yb addition.

3.2. Eutectic solidification behavior analysis

3.2.1. Thermal analysis

Fig. 6 shows an assembly of all cooling curves of Al–7.5%Si–0.45%Mg alloys with different Yb contents. The cooling curves of the unmodified and Sr modified alloys are also provided. The characteristic temperatures for the eutectic reactions from the cooling curves are shown in Table 2. Because the content of Yb in the alloy is low, the cooling curves do not show any peaks related to the formation of the Yb-containing phases.

It can be clearly observed in Fig. 6 and Table 2 that the formation of primary aluminum dendrite is not significantly changed with the addition of Sr or Yb. However, Sr or Yb additions cause an increase in recalescence at the eutectic temperature and a depression of the eutectic temperature, as commonly in the literature [14]. The nucleation temperature (T_N) of the unmodified alloy is 572.6 °C, and growth temperature is 569.8 °C. With the introduction of 0.15% Yb, the temperatures are decreased by about 6.8 °C and 5.2 °C, reaching 565.8 °C and 564.6 °C, respectively. Further increases in Yb content do not seem to alter the cooling curves significantly. Upon adding 0.04% Sr into the alloy, the eutectic nucleation temperature, growth temperature and recalescence are 565.4 °C, 563.7 °C and 0.8 °C, respectively.

3.2.2. Quenching analysis

Fig. 7 shows the typical micrographs of the quenched samples just after the commencement of eutectic solidification. Several regions of eutectic growth can be observed in all micrographs, with the quenched liquid showing a dark grey appearance. A typical sample containing 0.3% Yb was chosen for characterization in the quenching experiment. Fig. 7a–c show the low magnification micrographs of the quenched alloys, which can describe the nucleation frequency. A large number of eutectic grains are present in the unmodified alloy as seen in Fig. 7a. However, very few eutectic grains are observed in the quenched Yb or Sr modified sample

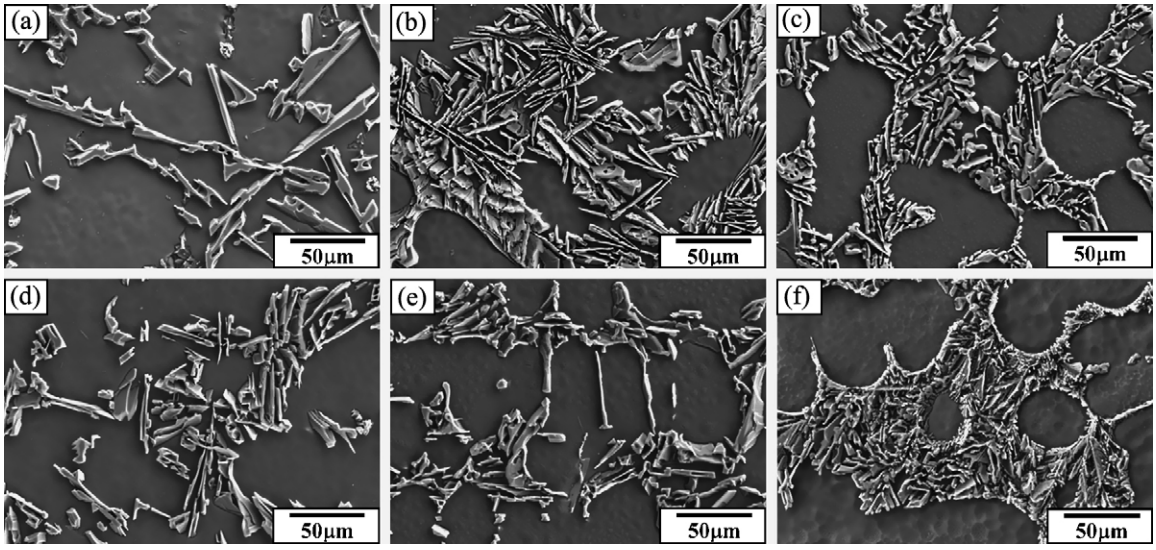

Fig. 4. High magnification morphology of silicon in Al–7.5%Si–0.45%Mg alloys: (a) unmodified, (b) 0.15% Yb, (c) 0.3% Yb, (d) 0.5% Yb, (e) 1.0% Yb and (f) 0.04% Sr.

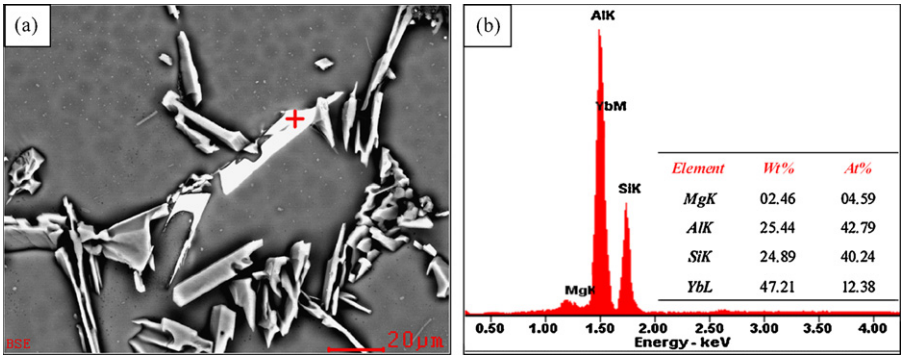

Fig. 5. SEM microstructure and EDS analysis of the Yb-containing phase in the 0.5% Yb modified alloy: (a) morphology and (b) EDS of the Yb-containing phase.

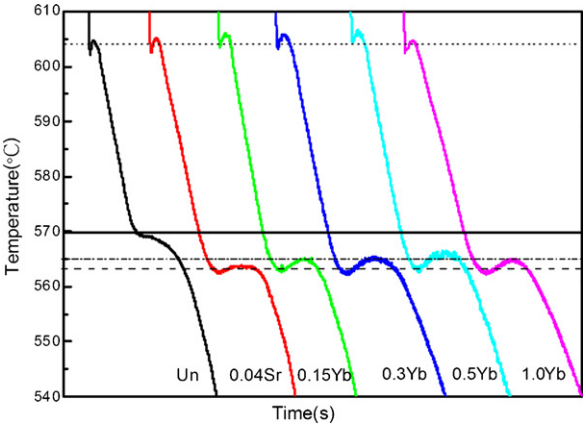

Fig. 6. Cooling curves of Al–7.5%Si–0.45%Mg alloys.

Table 2
Variation of characteristic temperatures of Al–7.5%Si–0.45%Mg alloys.

Alloys	T_N/°C	T_{Min}/°C	T_G/°C	Recalescence ΔT/°C
Un	572.6	–	569.8	0
0.04Sr	565.4	562.9	563.7	0.8
0.15Yb	565.8	563.0	564.6	1.6
0.3Yb	565.1	562.5	564.8	2.3
0.5Yb	566.6	563.0	565.6	2.6
1.0Yb	564.5	562.5	564.7	2.2

(Fig. 7b and c). It appears that the addition of Yb or Sr has reduced the number of eutectic grains that nucleate. The high magnification micrograph of the quenched unmodified alloy is shown in Fig. 7d, the eutectic is located at or close to the tips of the aluminum dendrites and tends to grow into the liquid with a very jagged solid–liquid interface. Fig. 7e and f show the high magnification quenched micrograph of the 0.3% Yb and 0.04% Sr modified samples, respectively. It is worthwhile emphasizing that the eutectic is not formed adjacent to the tips of dendrites, but instead centralized in the interdendritic region. At least, the connection with the primary phase appears less than that of the unmodified alloy.

4. Discussion

The addition of Yb gives rise to a refinement of the eutectic silicon in Al–7.5%Si–0.45%Mg alloy. Nevertheless, the modification effect is not dramatic compared with the Sr modified alloy. It is well established that modification of Al–Si eutectic is typically accompanied by a depression in the eutectic growth temperature, and a larger depression of the eutectic arrest temperature is related to increased modification [14]. It can be found that eutectic temperatures are all suppressed by the addition of Yb or Sr, as shown in

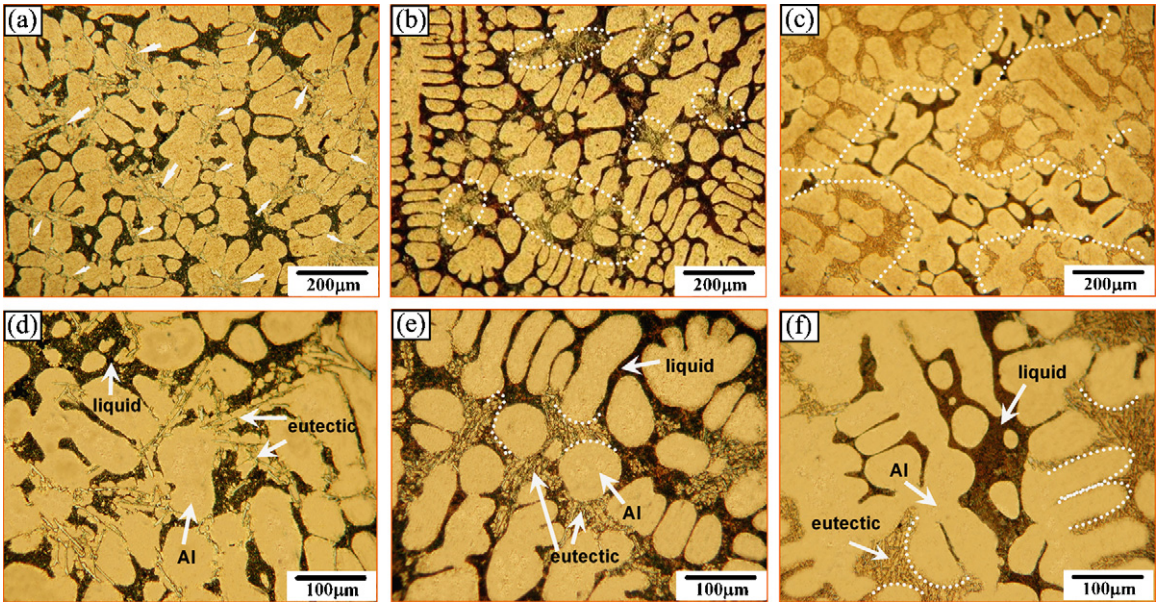

Fig. 7. Micrographs of the quenched Al–7.5%Si–0.45%Mg alloys: (a) and (d) unmodified, (b) and (e) 0.3% Yb and (c) and (f) 0.04% Sr.

Fig. 6 and Table 2. The reduction in eutectic growth temperature (T_G) of more than 5 °C is typical of that which occurs with modification [1], but only the Sr modified alloy exhibits a fine fibrous eutectic silicon structure. It indicates that even though a low eutectic temperature is a feature of the well-modified microstructure, there is no determinate relationship between silicon morphology and eutectic temperature [11,17,32].

Referring to the mechanism of IIT model, a value of about 1.65 is proposed as the ideal value for the ratio of atomic radius of modifier to that of silicon [21]. Yb with the optimum atomic ratio of 1.65 is therefore predicted to result in modification, since the radius ratio of Yb to Si is closer to the optimum than that of Sr (1.84). Lu and Hellawell [21] reported that the addition of 0.5% Yb resulted in a significant modification of eutectic silicon based on the twin observations. However, the introduction of Yb causes a refinement of eutectic silicon, and the structure is not the same as the fibrous modification with Sr addition in the present work. Investigations by Knuutinen et al. [14] and later by Nogita et al. [12] also found that even at the addition of 1.35% Yb, fibrous modification does not occur and the silicon is still plate-like, although it is somewhat refined. Therefore, we believe that Yb addition results in a fine plate-like structure which is not the same as the fibrous modification seen with Sr or Na additions. It should be noted that although twins are frequently observed in the modified silicon phase, the atomic radius ratio criterion is not always a universal law governing the modification of eutectic silicon. On the other hand, the addition may influence the nucleation kinetics in such a way by interaction with some other impurity, eliminating some heterogeneous sites in the liquid. Thereby, the reduced nucleation density is proposed to cause an increase in the growth rate because of the smaller solid–liquid interface area and modify the microstructure [27,34]. It is evident from Figs. 6 and 7 that the nucleation temperature and nucleation frequency of eutectic silicon are indeed reduced by the addition of Yb, which is similar to that of the Sr modified alloy. However, the modification still lags far behind, which is consistent with the literatures [32,35]. The increased interface velocity caused by reduced nucleation is not sufficient to cause a flake–fibrous transition, and the flake-to-fibre transition that occurs with impurity modification is shown to be independent of any change in eutectic nucleation mode and frequency. The different influence of Sr and Yb on modification is that Sr segregates exclusively to the eutectic silicon phase and affects growth of silicon [36], whereas Yb is not found in the silicon phases at all [12]. Therefore, modified growth rather than nucleation is thought to be the primary cause of the modification.

It should be noted that the eutectic silicon is some crystallographically very imperfect and able to bend and split to create a finer microstructure with a higher cooling rate (about 5 °C/s), compared with the early investigations (about 1 °C/s) [12,14]. We believe that the different modification of Yb can be attributed to the different cooling rate. However, further research is required to clarify and confirm the above phenomena in detail. It is likely that other modifying factors and modification parameters should be examined together carefully.

The size and interflake spacing of eutectic silicon in the Yb modified alloys are reduced, compared with the unmodified alloy. Roughly, there are two refinement mechanisms. One is nucleation behavior and another is undercooling. The heterogeneous nucleation mechanism is proposed to be the refinement mechanism of Sb in Al–Si alloys [10,37]. As for the refinement of eutectic silicon by Sb, it was proposed that Sb promotes the nucleation of silicon, resulting in a fine microstructure. However, the Yb-containing phase formed in the alloys may be $YbAl_2Si_2$, as shown in Fig. 5. In addition, other potential particles formed in the alloys are $YbAl_3$ and Yb_2AlSi_2. The lattice mismatch of all the particles with silicon is too large to be the ideal nucleation site of silicon [38,39]. Therefore, the Yb-containing phases cannot be taken as nucleation sites of eutectic silicon because of the lattice misfit, which is consistent with the results of cooling curves given in Fig. 6 and Table 2.

In this case, the reduction of the size and interflake spacing of eutectic silicon in the Yb modified alloys can be attributed to the undercooling during solidification. During the solidification process of Al–7.5%Si–0.45%Mg alloy, primary aluminum nucleates at the liquidus temperature, and then the dendrites start growing. Yb has a very low solubility either in Al or Si. During the growth of primary aluminum dendrite, Yb and Si elements are rejected by the advancing α-Al solid. Thus, the segregation at the front of the advancing solid–liquid interface results in an intensive constitutional undercooling, as thermal analysis does indeed show in Fig. 6 and Table 2. On the other hand, the undercooling also increases due to the reduction of nucleation with the addition of Yb. The increase of undercooling can restrict the growth of silicon phase during eutectic reaction. Therefore, the undercooling caused by the presence of Yb contributes to refining the silicon phase.

5. Conclusions

Addition of Yb can modify the eutectic silicon in Al–7.5%Si–0.45%Mg alloy, and structural transformation is limited to a refinement of the coarse plate-like silicon structure to a fine flake-like and some branched morphology. In addition, the formation of Yb-containing phases at higher content of Yb results in a deterioration of modification. The introduction of Yb decreases the temperatures of eutectic nucleation and growth. However, a single cooling curve is not sufficiently sensitive to make accurate predictions of modified structure. The quenching results reveal that the nucleation frequency is reduced with the addition of Yb. The eutectic is located at or adjacent to the primary phase in the unmodified alloy, whereas the eutectic has a tendency to evolve into interdendritic region in the modified alloys. The modified growth rather than nucleation is thought to be the primary cause of the modification, and the corresponding undercooling caused by the presence of Yb plays an important role in the refinement of eutectic silicon.

References

[1] J.E. Gruzleski, B.M. Closset, in: I.L. Schaumburg (Ed.), The Treatment of Liquid Aluminum–Silicon Alloys, American Foundrymen's Society, 1990.
[2] O.E. Sebaie, A.M. Samuel, F.H. Samuel, H.W. Doty, Mater. Sci. Eng. A480 (2008) 342–355.
[3] M.M. Makhlouf, H.V. Guthy, J. Light Met. 1 (2001) 199–218.
[4] O. Uzun, F. Yilmaz, U. Kölemen, N. Basman, J. Alloys Compd. 509 (2011) 21–26.
[5] C. Triveño Rios, M.M. Peres, C. Bolfarini, W.J. Botta, C.S. Kiminami, J. Alloys Compd. 495 (2010) 386–390.
[6] S. Zhang, Y. Zhao, X. Cheng, G. Chen, Q. Dai, J. Alloys Compd. 470 (2009) 168–172.
[7] Z. Zhang, J. Li, H. Yue, J. Zhang, T. Li, J. Alloys Compd. 484 (2009) 458–462.
[8] W. Jie, Z. Chen, W. Reif, K. Müller, Metall. Trans. A34 (2003) 799–806.
[9] X. Bian, W. Wang, Mater. Lett. 44 (2000) 54–58.
[10] A.K. Prasada Rao, K. Das, B.S. Murty, M. Chakraborty, Mater. Lett. 62 (2008) 2013–2016.
[11] Y.C. Tsai, C.Y. Chou, S.L. Lee, C.K. Lin, J.C. Lin, S.W. Lim, J. Alloys Compd. 487 (2009) 157–162.
[12] K. Nogita, H. Yasuda, M. Yoshiya, S.D. McDonald, K. Uesugi, A. Takeuchi, Y. Suzuki, J. Alloys Compd. 489 (2010) 415–420.
[13] K. Gammer, E. Ogris, P.J. Uggowitzer, H. Hutter, Microchim. Acta 141 (2003) 23–27.
[14] A. Knuutinen, K. Nogita, S.D. McDonald, A.K. Dahle, J. Light Met. 1 (2001) 229–240.
[15] K. Nogita, A. Knuutinen, S.D. McDonald, A.K. Dahle, J. Light Met. 1 (2001) 219–228.
[16] B. Li, H. Wang, J. Jie, Z. Wei, Mater. Des. 32 (2011) 1617–1622.
[17] W. Prukkanon, N. Srisukhumbowornchai, C. Limmaneevichitr, J. Alloys Compd. 477 (2009) 454–460.
[18] D. Emadi, A.K.P. Rao, M. Mahfoud, Mater. Sci. Eng. A527 (2010) 6123–6132.
[19] S.H.K.N. Prabhu, J. Mater. Sci. 43 (2008) 3009–3027.
[20] H.S. Kang, W.Y. Yoon, K.H. Kim, M.H. Kim, Y.P. Yoon, I.S. Cho, Mater. Sci. Eng. A449–451 (2007) 334–337.
[21] S.Z. Lu, A. Hellawell, Metall. Trans. A18 (1987) 1721–1733.

[22] J.Y. Chang, H.S. Ko, J. Mater. Sci. Lett. 19 (2000) 197–199.
[23] K. Nogita, J. Drennan, A.K. Dahle, Mater. Trans. 44 (2003) 625–628.
[24] P. Srirangam, M.J. Kramer, S. Shankar, Acta Mater. 59 (2011) 503–513.
[25] S. Shankar, Y.W. Riddle, M.M. Makhlouf, Metall. Mater. Trans. A35 (2004) 3038–3043.
[26] S. Shankar, Y.W. Riddle, M.M. Makhlouf, Acta Mater. 52 (2004) 4447–4460.
[27] A.K. Dahle, K. Nogita, J.W. Zindel, S.D. McDonald, L.M. Hogan, Metall. Mater. Trans. A32 (2001) 949–960.
[28] K. Nogita, A.K. Dahle, Mater. Charact. 46 (2001) 305–310.
[29] S.D. McDonald, K. Nogita, A.K. Dahle, J. Alloys Compd. 422 (2006) 184–191.
[30] X. Song, X. Bian, J. Zhang, J. Zhang, J. Alloys Compd. 479 (2009) 670–673.
[31] M. Asta, C. Beckermann, A. Karma, W. Kurz, R. Napolitano, M. Plapp, G. Purdy, M. Rappaz, R. Trivedi, Acta Mater. 57 (2009) 941–971.
[32] S.D. McDonald, K. Nogita, A.K. Dahle, Acta Mater. 52 (2004) 4273–4280.
[33] H. Baker, H. Okamoto, Alloy phase diagrams, in: ASM Metals Handbook, vol. 3, ASM Int., Ohio, 1992.
[34] S.C. Flood, J.D. Hunt, Met. Sci. 15 (1981) 287–294.
[35] M.D. Hanna, S.Z. Lu, A. Hellawell, Metall. Mater. Trans. A15 (1984) 459–469.
[36] K. Nogita, H. Yasuda, K. Yoshida, K. Uesugi, A. Takeuchi, Y. Suzuki, A.K. Dahle, Scripta Mater. 55 (2006) 787–790.
[37] B. Xiufang, W. Weimin, Q. Jingyu, Mater. Charact. 46 (2001) 25–29.
[38] C. Kranenberg, D. Johrendt, A. Mewis, Z. Anorg. Allg. Chem. 625 (1999) 1787–1793.
[39] C. Kranenberg, A. Mewis, Z. Anorg. Allg. Chem. 626 (2000) 1448–1453.